

CHARACTERISTIC LOAD CASES OF BIAXIAL BRAIDS

D. Michaelis and P. Middendorf

Institute of Aircraft Design (IFB), University of Stuttgart,

Pfaffenwaldring 31, 70569 Stuttgart, Germany

Emails: michaelis@ ifb.uni-stuttgart.de, middendorf@ifb.uni-stuttgart.de,

Web Page: <http://www.ifb.uni-stuttgart.de>

Keywords: braiding, testing, damage, strain field, micro-graphs

Abstract

Two-dimensional biaxially braided composites exhibit a complex damage behaviour. It can be highly non-linear and is dependent on the type and orientation of the loading.

In this paper, different carbon fibre/epoxy specimens (braiding angle $\beta = \pm 30^\circ$ and $\pm 55^\circ$) are tested in tension and compression. Two characteristic load cases resulting in different strain distributions relative to the fibres are identified by examining the damage behaviour; in load case 1 failure is triggered by shear, while in load case 2 failure is dominated by cross-fibre tension.

The paper is structured into three parts. In part I, the definition of the characteristic load cases are given. Part II is the analysis of an extensive test campaign, compromising compression and tension tests in longitudinal and transverse direction. The third part is the validation of the characteristic load cases by identifying the characteristic damage done in the prevailing load case using different measurement techniques: optical 3D deformation recordings and micro-graphs.

The conclusion is that the knowledge about the two loading cases can be used in the characterisation of biaxial braids, as it is important to be sure to test both loading cases adequately.

1. Introduction

Composite materials can be manufactured using a multitude of technologies. One method, which is well-suited for long and slender parts, is biaxial braiding. The created textile structure has non-linear mechanical properties which are not well understood, compared to conventional non-crimp fabrics (NCF). They are dependent on both the braiding angle of the fibres as well as the direction of the load. This makes it a complex issue to describe the damaging and failure behaviour in a universally valid way.

The goal of this paper is to show patterns in the stress-strain-curves for both tension and compression tests in both longitudinal and transverse direction. Two “characteristic load cases” can be identified which help to simplify the way biaxially braided carbon fibre composite materials (“biaxial braids”) can be described and modelled.

2. Basics of braiding and testing

A braid is a textile structure which is created by interlacing yarns (fibre bundles). They are guided on sinusoidal rotational paths, creating a sleeve. If a mandrel is placed in the centre of this sleeve during its manufacturing process, a near net-shaped preform is created as the newly formed braid contracts onto the mandrel (see Fig. 1). Of course, a mandrel of suitable diameter and geometry is essential.

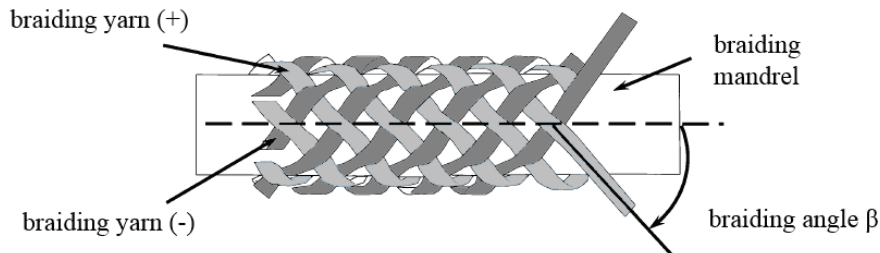


Figure 1. Schematic illustration of a biaxial braid [1].

The angle formed between the centre line of the braid sleeve and the braiding yarns is called the braiding angle β . It is dependent on the mandrel diameter d , the angular frequency ω_b of the braiding yarns and the axial mandrel speed v_a , see Eq. 1.

$$\beta = \tan^{-1} \left(\frac{d \cdot \omega_b}{2 \cdot v_a} \right) \quad (1)$$

The textile structure of a braid varies for different braiding angles, which usually lie between 30° and 60°. For braids without gaps, a smaller β results in wider and flatter yarns, compared to a braid with a bigger β (on the same mandrel, see Fig. 2). This leads to a variation in yarn undulation: the amplitude of the sinusoidal path of a yarn crossing over and under another yarn gets bigger as the thickness of the yarns increases. As a result, the in-plane stiffness of the final composite material is reduced.

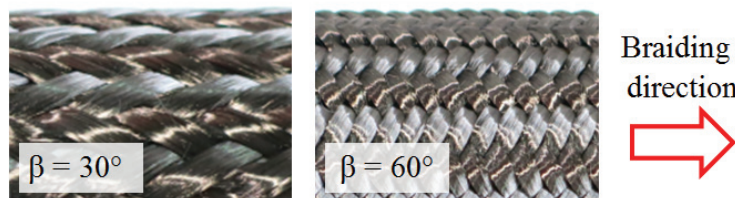


Figure 2. Differences in the textile structure can be seen for different braiding angles.

This work focuses exclusively on two-dimensional braids. In order to create a larger material thickness, several layers have to be placed onto each other. Unlike in three-dimensional braids, there is no interlock between layers. However, a “nesting effect” occurs [1], which means that the individual braid layers overlap locally in thickness direction. This causes an improved impact performance, in comparison to NCF composites [2].

In order to get a reliable and reproducible braiding result, a programmable industrial robot (e.g. by KUKA Roboter GmbH, Augsburg, Germany) is used to guide the mandrel through the center of the braiding machine during operation, see Fig. 3. At IFB, a radial braiding machine with 176 braiding bobbins is used, of type RF 1/176-100 by August Herzog Maschinenfabrik GmbH & Co. KG, Oldenburg, Germany. The yarns used are HTS40 12k Z0 by Toho Tenax GmbH, Wuppertal, Germany. They are composed of 12.000 carbon fibres and have a titer of 800 tex (g/km).

The final preform is then infiltrated with epoxy resin using vacuum assisted resin infusion (VARI), similar to Fig. 4. The resin used is MGS RIM 135 with the hardener MGS RIMH 1366 by Hexion Speciality Chemicals GmbH, Stuttgart, Germany.

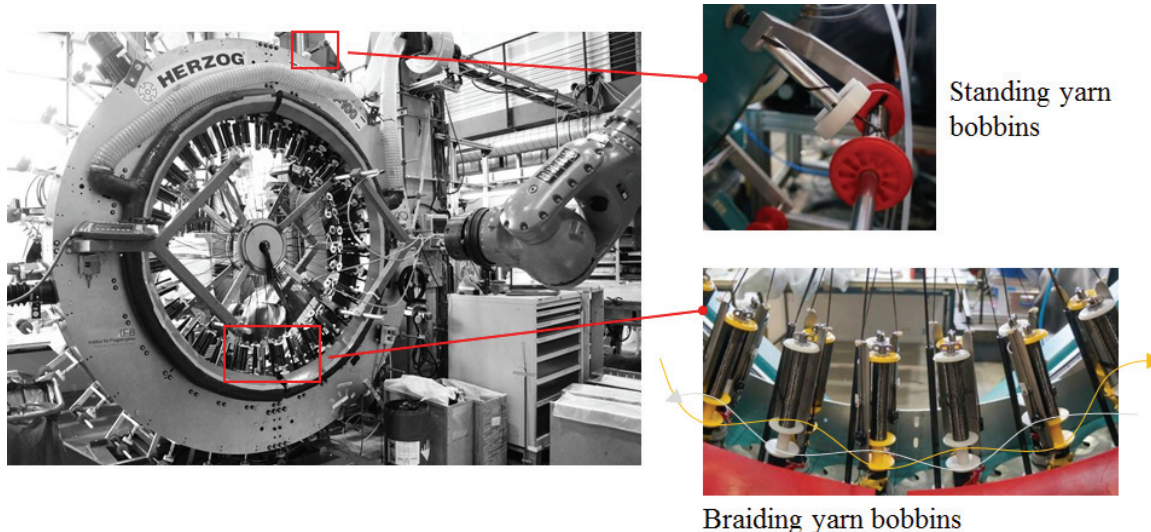


Figure 3. Automated braiding set-up at the Institute of Aircraft Design (Institut für Flugzeugbau) [3].

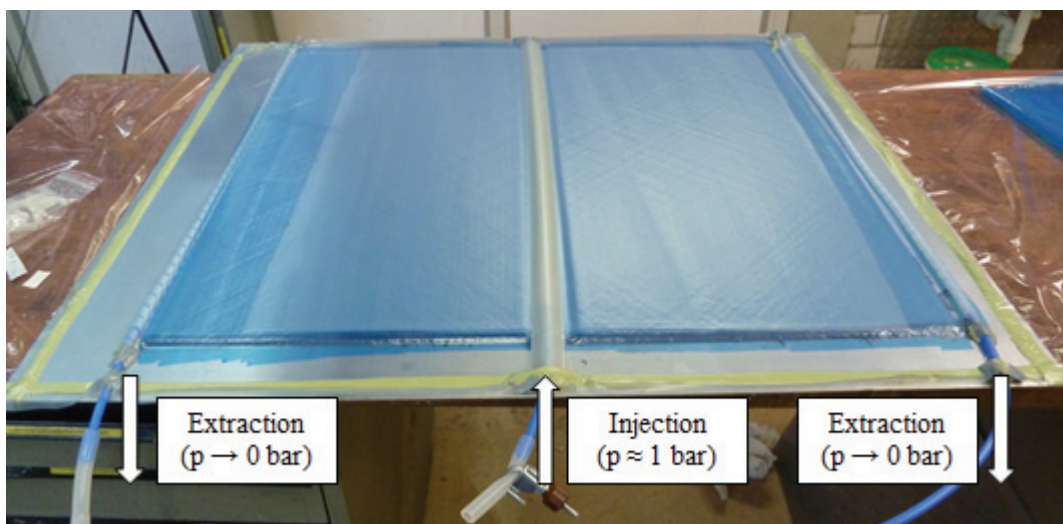


Figure 4. Example of a vacuum resin infusion of a braided tube [4].

Because the unit cell of a braid with 12k-yarns are large (width of up to 19,7 mm), a testing standard was chosen which has a large specimen width. The Airbus Test Methods AITM 1-0007 (for tension) and AITM 1-0008 (for compression) describe specimens with a width of 32 mm and are suitable for braided composite materials. The manufacturing of the specimens is as follows: eight layers are individually braided onto a mandrel with a diameter of 120 mm and longitudinally cut into a rectangle and stacked. The stack is then infiltrated and cured. After the tabs are bonded onto the final specimen geometry can be cut. The gauge length is 180 mm for the tension test specimens and 32 mm for the compression test specimens, see Fig. 5. The tests are carried out on a universal testing machine by company Schenck-Trebel, Wuppertal, Germany.

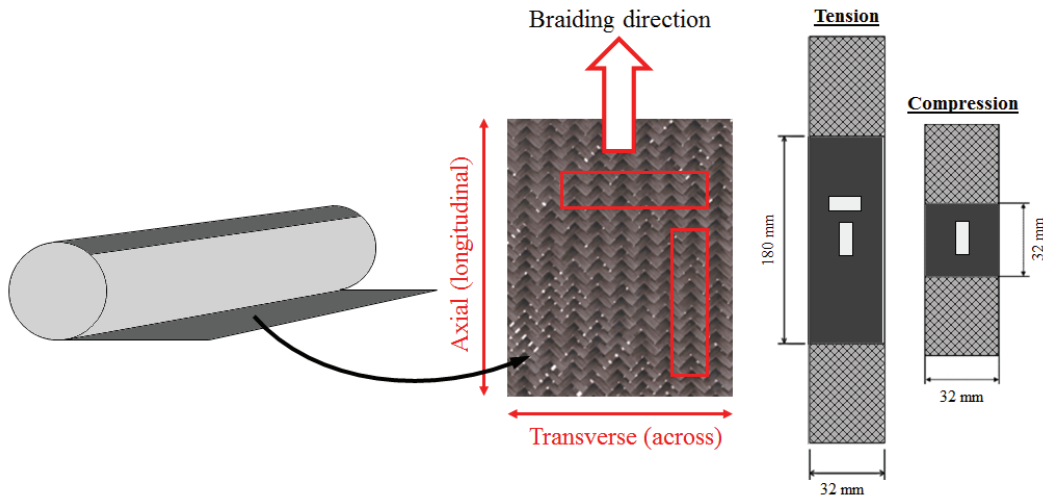


Figure 5. The individual braid layers are removed from the mandrel (left); after infiltration and curing, the specimens are cut from the board (centre); for tension and compression tests, the specimen sizes are shown, including the rough position of the strain gauges (right).

3. Hypothesis and method

Based on the initial motivation, the lack of a simple way to describe the seemingly complex, direction-dependent behaviour of braids, a hypothesis is formulated: *The direction-dependend mechanical behaviour of biaxial braids can be described using two “characteristic load cases”*.

This hypothesis is to be tested in a three-step procedure: on the basis of a new formulation for characteristic load cases (part I) an extensive test campaign is analysed qualitatively (part II) and metrologically validated (part III).

4. Part I: Formulation of characteristic load cases

In the following, the theoretical concept of the two characteristic load cases, valid for tension and compression, is described. Important is the definition of the “smaller fibre angle” β_{\min} , which is of the value of the braiding angle or its complementary angle, whichever is smaller (see Eq. 2). The “bigger fibre angle” β_{\max} is the complementary angle to β_{\min} . The different load cases always apply to β_{\min} .

$$\beta_{\min} = \min(\beta, 90^\circ - \beta) \quad (2)$$

$$\beta_{\max} = 90^\circ - \beta_{\min} \quad (3)$$

In Fig. 6, the two load cases are shown schematically:

- In “load case 1”, either a compressive load is applied at β_{\max} or a tensile load at β_{\min} . Due to the Poisson effect, a positive shear acts on β_{\min} . This results in compression across and tension along the braiding yarns.
- In “load case 2”, either a tensile load is applied at β_{\max} or a compressive load at β_{\min} . Due to the Poisson effect, a negative shear acts on β_{\min} . This results in tension across and compression along the braiding yarns.

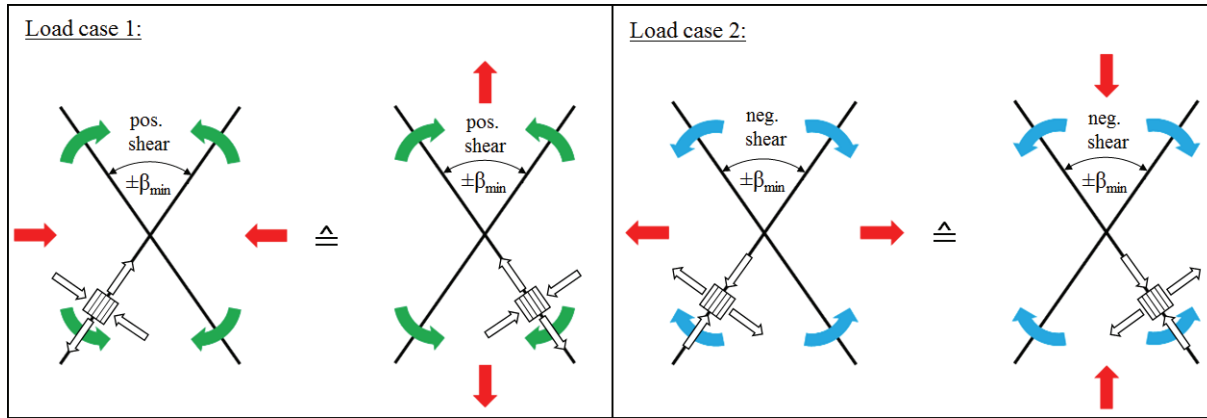


Figure 6. In load case 1, there is compression across and tension along the braiding yarns (left). In load case 2, there is tension across and compression along the braiding yarns (left).

In principle, it is therefore not relevant for the type of strain acting on the fibres in the braiding yarns, if the global loading force is compressive or tensile. The local coordinate system is rotated to fit the braiding yarn direction, which is identical to the local layerwise orientations in analytical or numerical calculations.

From the analytical model above the conclusion is drawn that the behaviour of the braid does not depend on the real physical braiding angle, but only on the resulting fibre angles (β_{\min} and β_{\max}). Stiffness-reducing effects due to different undulations are not taken into account. The following assumption is therefore made: *The behaviour of two complementary biaxial braids is identical, i.e. the axial tensile behaviour of „Biax β “ is the same as the transverse tensile behaviour of „Biax 90°- β “, despite differences in textile structure.* This leads to the introduction of the effective fibre angle β_{eff} , onto which the acting force is applied, see Fig. 7.

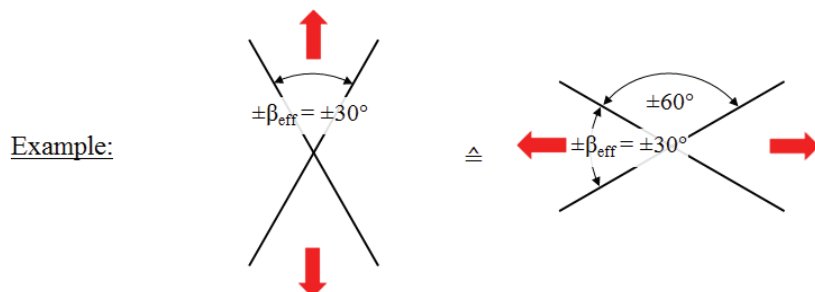


Figure 7. Example for the use of the effective fibre angle β_{eff} for Biax 30° and Biax 60°.

5. Part II: Analysis of test campaign

A test campaign was executed in order to get a comprehensive understanding of the mechanical behaviour of biaxial braids. The test matrix is shown in Tab. 1. As six specimens were tested for each configuration, the total number of tests is 48. The meaning of the notations axial and transverse are illustrated in Fig. 5.

Table 1. Test matrix for Biax 30° and Biax 55°, composed of tensile and compressive tests in axial and transverse material direction.

Test matrix		Tension	Compression
Biax 30°	axial	✓	✓
	transverse	✓	✓
Biax 55°	axial	✓	✓
	transverse	✓	✓

An analysis of the tension and compression tests shows a similar qualitative and quantitative behaviour for similar effective fibre angles ($\beta_{\text{eff}} = 30^\circ, 35^\circ, 55^\circ$ and 60°), despite differences in textile structure between Biax 30° and Biax 55°. It can be concluded that the internal textile structure has little effect on the overall stress-strain-curves. However, there is a smaller impact to be expected on e.g. the exact value on the Young's moduli.

Fig. 8 shows that the stress-strain-curves can be split into two groups for both the tensile and the compressive tests. These two categories correspond to the two load cases. This is a strong indicator that the concept of examining the behaviour of biaxial braids via loading is reasonable.

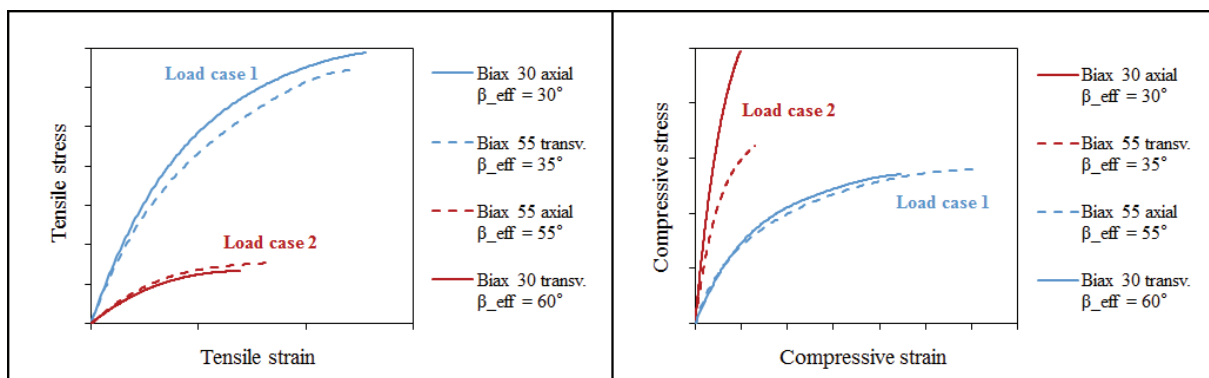


Figure 8. Representative stress-strain-curves for tensile (left) and compressive (right) tests on braids Biax 30° and Biax 55°. The curves are labeled with their respective load case.

6. Part III: Metrological validation

In the following, the characteristic load cases are validated metrologically. First, the strain fields on the surface of tensile specimens are analysed. The goal is to show that the tension and compression along and across the braiding yarns exists like predicted in part I. Then, an attempt is made to observe the progression of damage mechanisms inside the material, using micro-graphs. The validation is performed using tensile specimens of type Biax 30°, Biax 45° and Biax 55°.

6.1 Optical deformation analysis

The optical measurement system ARAMIS by GOM mbH, Braunschweig, Germany is used to measure the in-plane deformation at the surface of a specimen. For the system to work, a black-on-white stochastic spot pattern pattern is sprayed onto the specimen surface. This surface is tracked by a stereo camera, allowing the movement of the spots to be tracked. During the tensile tests, one image per second is recorded for a later further processing. For the analysis of the deformation field, the reference coordinate system is rotated to fit the braiding angle. This way, the strain is calculated relative to the braiding yarns for the additional tension specimens of type “Biax 30° axial” and “Biax 55° axial”.

In Fig. 9 it is shown that the strain field varies locally, with bigger strains in resin-rich areas like inbetween yarn and smaller strains in yarns. This way, the textile structure of the composite can be seen. The strain across the braiding yarns (ε_y) is presented exemplarily, also because it is important for damage progression (and damage modelling in simulations) whether it is positive or negative. On the left in Fig. 9, an example for load case 1 can be seen and the peak for ε_y lies at about -1,2% (compression). On the right, an example for load case 2 is shown with the peak at about +0,6% (tension). This agrees with the prediction in part I and therefore validate the theoretical concept of characteristic load cases.

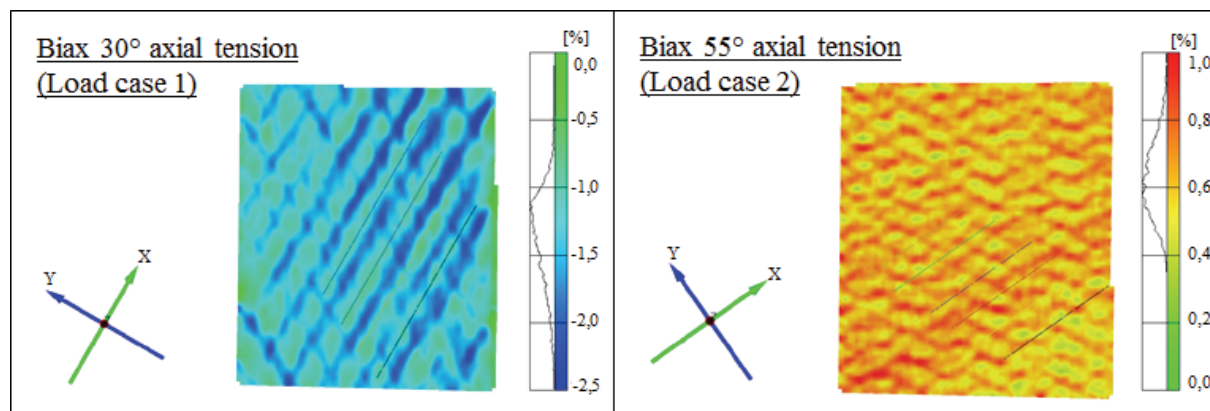


Figure 9. Strain field perpendicular to one braiding yarn direction (ε_y) for tension specimens of type Biax 30° axial (left) and Biax 55° axial (right).

6.2 Micro-graphs

Leaving the macroscopic (part II, ch. 5) and the mesoscopic scale (part III, ch. 6.1), the damage progression inside the material is considered on a microscopic scale. The method is to cut specimens along the braiding yarns (i.e. $\pm 30^\circ$, $\pm 45^\circ$ or $\pm 55^\circ$ off the braiding direction) and to create micro-graphs at different damaging stages. In order to test this approach, a series of tensile specimens of type Biax 45° axial is examined at the stages: undamaged (0% of breaking load), partly damaged (90% of breaking load) and after failure (100% of breaking load). The micro-graphs for the damaged specimens are generated at the location of visible damage in order to get the best results.

The material type Biax 45° lies on the border between the two load cases. However, it can be sensibly used to verify this method for the observation of damage progression. In Fig. 10 the differences in three similar areas within the braid are compared using two different magnifications (25x and 100x). It can be seen that in the undamaged state, resin-rich separate the yarns. In the partly damaged state, micro-cracks have propagated perpendicularly through the yarns. And at failure, the material fractures mainly inbetween yarns, leaving wide cracks. This shows that micro-graphs are a valid method to observe and compare damage progress in biaxial braids.

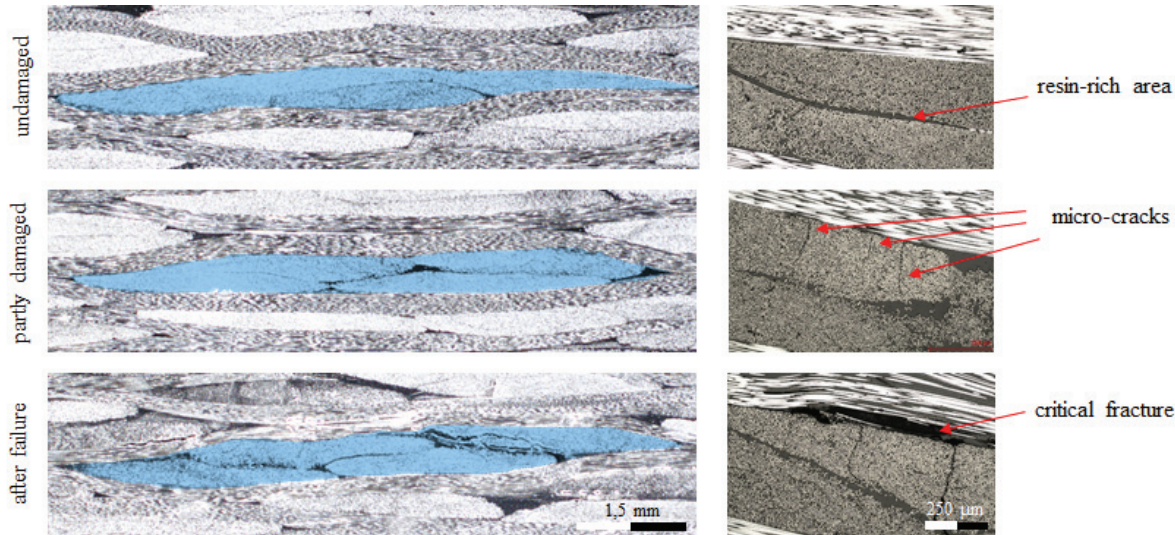


Figure 10. Micro-graphs of tensile specimens of type Biax 45° axial. Comparable areas are coloured blue (left), a further magnified detail is shown on the right.

7. Summary and conclusion

A novel concept to examine the damage behaviour of biaxially braiding carbon fibre composites under quasi-static load is presented. With the help of characteristic load cases, the complex material response is simplified and divided into two cases. A hypothesis stating this is formulated.

In part I, these load cases are introduced and defined theoretically. A central aspect is the algebraic sign of the strain across the braiding yarns, which influences the damage progression. In part II, an extensive testing campaign on Biax 30° and Biax 55° is analysed and patterns are found in the stress-stress-curves which support the hypothesis. In part III, two different metrological techniques are used to validate the existence of the load cases. Here, the optical recording of the strain field show strong supporting evidence, while micro-graphs can be shown to be well-suited for more detailed future research.

References

- [1] Birkefeld, K.; Röder, Mirko; Reden, Tjark; Bulat, M.; Drechsler, K. (2012): Characterization of Biaxial and Triaxial Braids: Fiber Architecture and Mechanical Properties. In: Applied Composite Materials 19
- [2] Wagner, H.; Bansemir, H.; Drechsler, K.; Weimer, C. (2007): Impact behavior and residual strength of carbon fiber textile based materials. In: 3rd SAMPE Europe Technical Conference.
- [3] Michaelis, D.; Prinz, N.; Krauter, A.; Middendorf, P. (2015): Evaluation of compressive test methods for braided composites using coupon and tube specimens. In: 18th International Conference on Composite Structures.
- [4] Rieckhoff, B. (2013): Experimentelle Charakterisierung und Interpretation der mechanischen Eigenschaften von CFK-Geflechten. Student project at Institute of Aircraft Design at University of Stuttgart.